2012

Optical properties of cobalt slanted columnar thin films passivated by atomic layer deposition

Daniel Schmidt
University of Nebraska-Lincoln, schmidt@huskers.unl.edu

Eva Schubert
University of Nebraska-Lincoln, efranke3@unl.edu

Mathias Schubert
University of Nebraska-Lincoln

Optical properties of cobalt slanted columnar thin films passivated by atomic layer deposition

Daniel Schmidt,[a] Eva Schubert, and Mathias Schubert
Department of Electrical Engineering and Nebraska Center for Materials and Nanoscience,
University of Nebraska-Lincoln, Lincoln, Nebraska 68588-0511, USA

Optical properties of passivated metal slanted columnar thin films from cobalt within the visible spectral region are reported. Glancing angle deposition is utilized to grow slanted nanocolumns which have been conformally coated with Al_2O_3 by a subsequent atomic layer deposition process. A generalized anisotropic Bruggeman effective medium approximation has been employed to analyze spectroscopic generalized ellipsometry data. The modified homogenization approach allows for determination of biaxial (monoclinic) optical and structural properties as well as fractions of three film constituents. The conformal alumina passivation layer preserves the pristine metal character of the nanostructures and prevents oxidation and aging effects. © *2012 American Institute of Physics*. [doi:10.1063/1.3675549]

Three-dimensionally shaped metal sculptured thin films made by glancing angle deposition (GLAD) resemble an artificial material class with interesting physical properties.[1] However, in order to exploit optical and magneto-optical (magnetic) properties for possible applications, the as-deposited intrinsic material characteristics such as conductivity or ferromagnetic properties need to be preserved.[2,3] Hence, a thin homogeneous passivation shell is desired to especially prevent alterations due to material oxidation. It has been shown that atomic layer deposition (ALD) is an excellent technique to conformally coat complex nanostructures and sculptured thin films.[4,5]

In general, the characterization of material properties and quantification of material fractions of complex anisotropic thin films is a challenge. Non-destructive optical investigations, in particular, generalized ellipsometry is an excellent technique for probing anisotropic physical properties. However, the indirect method requires adequate mathematical model descriptive systems to match experimentally acquired data sets. Previously, an anisotropic Bruggeman effective medium approximation (AB-EMA) was employed to determine optical properties of metal slanted columnar thin films (SCTFs) in the visible spectral range. However, models were limited to uniaxial[6] or orthorhombic descriptions with a maximum of two different constituents.[7–9] Recently, we have shown that such an AB-EMA approach also leads to a very good approximation of structural and physical properties of anisotropic Co SCTFs in the THz spectral range.[10]

In this letter, we focus on the determination and quantification of a thin conformal Al_2O_3 layer on top of Co nanocolumns. It is evaluated how the alumina layer serves as a passivation layer thereby preserving the as-deposited optical properties of the Co SCTF. An augmented AB-EMA optical model approach is introduced to accurately describe the anisotropic optical response within the visible spectral range of a thin film comprising three material constituents (Co, Al_2O_3, and air). This approach leads to the determination of

structural parameters in excellent agreement to complementary techniques and reference samples.

Slanted nanocolumns from cobalt were deposited by electron-beam GLAD in a custom-built ultra-high vacuum chamber onto a low-doped n-type (001) silicon substrate at a deposition angle of 85°. Details about the growth process can be found elsewhere.[11] Immediately after the growth process, the sample was transferred to the ALD reactor (Fiji 200, CambridgeNanoTech Inc.). The subsequent thermal Al_2O_3 process[12] of 60 cycles was carried out at a substrate temperature of 60 °C in order to avoid sample property alterations by annealing effects. Both precursors, trimethylaluminum and nanopure water, were pulsed at 60 ms each followed by a 30 s purge time, which warrants a homogeneous and conformal coating of the columns with an aspect ratio of approximately 9. Note that even though ALD is a well-known technique to achieve highly conformal coatings of high aspect ratios, the uniformity is affected by non-ideal sample areas where columns are partially in contact. A schematic drawing of the final core-shell nanocolumnar thin film as well as cross-section scanning electron microscope (SEM) micrographs before and after ALD are depicted in Fig. 1. In order to determine the Al_2O_3 layer thickness, a 100 nm thick solid Co reference sample has been coated under identical ALD conditions. The resulting growth per cycle for the first 60 cycles determined with ellipsometry was 0.548 Å. Optical constants of transparent ALD grown Al_2O_3 have been determined prior to this investigation from an 18 nm thick layer with the Cauchy dispersion model. Angle-resolved spectroscopic Mueller matrix ellipsometry measurements were performed within a spectral range from 400 to 1000 nm (M2000VI, J. A. Woollam Co. Inc.). Spectra were taken at four different angles of incidence $\Phi_a = 45°$, 55°, 65°, and 75°, while performing a full sample rotation $0° \leq \phi \leq 360°$ in steps of 6°.

The experimentally acquired Mueller matrix spectra were analyzed with an augmented EMA approach based on the Bruggeman formalism.[13] EMAs are physical models based on the properties and the relative fractions of its

[a]Electronic mail: schmidt@huskers.unl.edu.

(a)

(b)

as-deposited
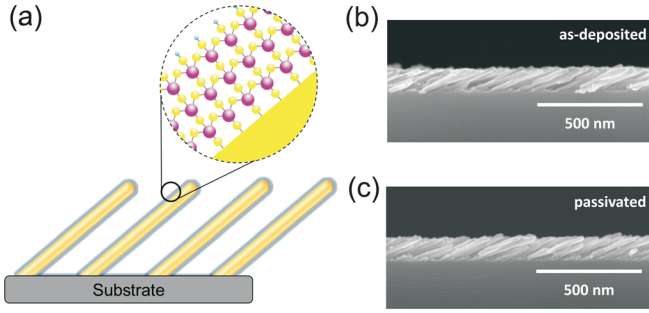
500 nm

(c)

passivated

500 nm

FIG. 1. (Color online) Schematic drawing of a core-shell Co SCTF coated with an Al_2O_3 passivation layer (3 ALD cycles depicted, (a)). High-resolution cross-section SEM micrographs reveal the structural equivalence before (b) and after (c) the ALD passivation process.

components and describe the macroscopic properties of a medium. The Bruggeman formalism, originally developed for spherical inclusions, is a homogenization process with absolute equality between the phases in mixture. An extension to randomly oriented anisotropic inclusions was obtained by introducing ellipsoidal depolarization factors L_a^D, L_b^D, L_c^D, representative for the inclusions' polarization along major polarizability axes **a**, **b**, and **c**.[14] The mixture macroscopically exhibits an isotropic effective polarizability $\langle P_{eff} \rangle$ with a single (isotropic) effective dielectric function ε_{eff} due to an averaging over all major polarizability axes (Fig. 2(a)). For spatially aligned inclusions of equal shape embedded in a host matrix (Fig. 2(b)), biaxial (orthorhombic) effective dielectric functions $\varepsilon_{eff,a}$, $\varepsilon_{eff,b}$, and $\varepsilon_{eff,c}$ are obtained along **a**, **b**, and **c**, respectively, instead of their average over all three semiaxes.[6–8] The anisotropic Bruggeman EMA (AB-EMA) formulae for the three effective major dielectric functions $\varepsilon_{eff,j}$ with $j = a,b,c$ for a mixture of m constituents in implicit form are

$$\sum_{n=1}^{m} f_n \frac{\varepsilon_n - \varepsilon_{eff,j}}{\varepsilon_{eff,j} + L_j^D(\varepsilon_n - \varepsilon_{eff,j})} = 0, \quad (1)$$

with the constraint that the sum of all material fractions f_n equals unity. ε_n is the dielectric function of the respective bulk material. L_j^D are the depolarization factors along the three orthogonal major polarizability axes **a, b, c**, and the sum of all three depolarization factors must obey unity $(L_a^D + L_b^D + L_c^D = 1)$.[14,15] Note that in order to preserve the symmetry of the original Bruggeman theory, structural
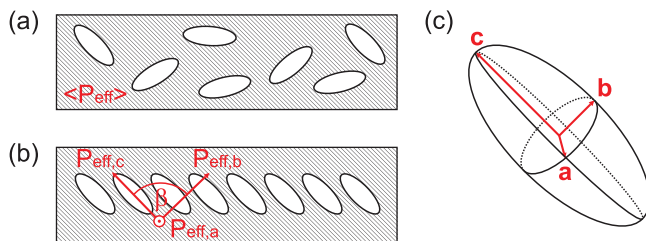
(a)

(b)

(c)

FIG. 2. (Color online) Effective medium scenarios with mixtures of ellipsoidal inclusions (general case) and a homogeneous host medium. The mixture with randomly oriented inclusions (a) exhibits an average effective polarizability $\langle P_{eff} \rangle$ whereas the mixture with aligned inclusions (b) shows anisotropic properties with three effective polarizabilities $P_{eff,j}$. The major polarizability axes system rendering the biaxial nature of the film is depicted in (c).

equivalence between constituents is assumed (one set of L_j^D renders the effective medium geometry).

A real-valued rotation matrix **A** with wavelength-independent Euler angles ϕ, θ, ψ can then be found to transform the Cartesian laboratory coordinate frame into the material coordinate frame.[16]

As reported previously, considering the ensemble of slanted columns, the film exhibits monoclinic optical properties such that $P_{eff,b}$ is not parallel to the semiaxis b of the ellipsoid but rather tilted towards c by a monoclinic angle β.[11,17,18] In order to describe biaxial materials with a monoclinic system, the obtained virtual orthogonal basis from Eq. (1) $(\varepsilon_{eff,j} = \varepsilon_j)$ has to be transformed by a projection matrix **U**:[19]

$$\varepsilon_m = U \begin{pmatrix} \varepsilon_a & 0 & 0 \\ 0 & \varepsilon_b & 0 \\ 0 & 0 & \varepsilon_c \end{pmatrix} U^T \quad \text{with} \quad U = \begin{pmatrix} 1 & 0 & 0 \\ 0 & \sin\beta & 0 \\ 0 & \cos\beta & 1 \end{pmatrix}, \quad (2)$$

where β is the monoclinic angle between axes **b** and **c**.

Best-match model calculations are carried out by simultaneously varying relevant model parameters (see Table I) in order to match model calculated data as closely as possible to the experimental data sets.

Two measurements of the same sample (Co SCTF passivated with a thin Al_2O_3 coating) are compared, which have been conducted both immediately after deposition and again 60 d later. The stratified optical model is composed of three layers accounting for Si substrate, native SiO_2, and an AB-EMA layer for the SCTF. The best-match model parameters within the AB-EMA layer for both measurement scenarios are summarized in Table I (Ref. 20) and respective wavelength-by-wavelength determined optical constants depicted in Fig. 3.

The AB-EMA layer of the Al_2O_3 passivated Co SCTF comprises bulk-like optical constants of three constituents: Co (model parameters), Al_2O_3, and void ($n = 1$, $k = 0$). Notably, except for material fractions, all best-match model parameters are virtually identical between measurements taken on the day of deposition and 60 d thereafter, respectively.

TABLE I. Overview of the best-match model parameters for both measurement scenarios, after deposition (0d) and 60 days later (60d), respectively, for the passivated Co SCTF. $t =$ thickness; $\theta =$ tilting angle with respect to the substrate normal; $\beta =$ monoclinic angle between axes c and a; $f_x =$ volume fraction of x; $L_j^D =$ depolarization factor along j. The error limits given in parentheses denote the uncertainty of the last digit (90% reliability).

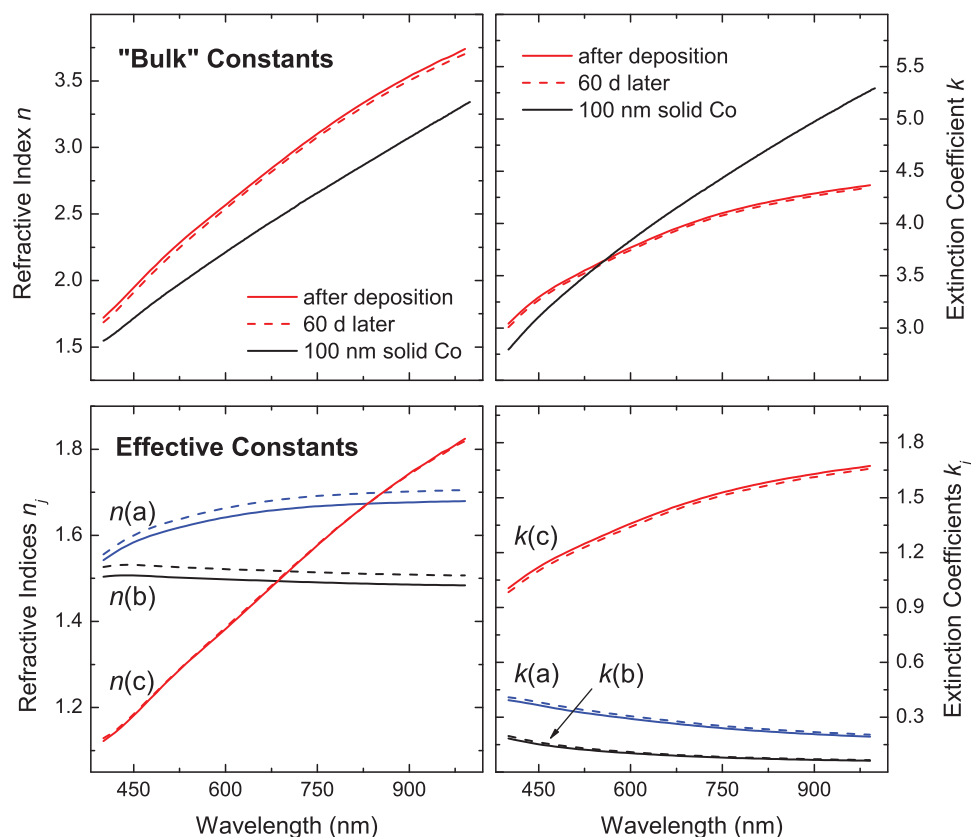| Parameter	Co + Al_2O_3 (after deposition)	Co + Al_2O_3 (60 d later)
t (nm)	89.46(3)	89.86(3)
θ (°)	62.69(1)	62.80(1)
β (°)	82.96(2)	83.39(2)
f_{void} (%)	62.03(7)	59.33(6)
$f_{Al_2O_3}$ (%)	13.98(8)	16.74(6)
L_a^D	0.4035(2)	0.4030(2)
L_b^D	0.5267(2)	0.5283(2)
L_c^D	0.0698(7)	0.0688(6)
MSE	8.45	10.82

FIG. 3. (Color online) Wavelength-by-wavelength determined optical constants for our Al_2O_3 passivated Co SCTF measured immediately after deposition (solid lines) and 60 days later (dashed lines), respectively. The first row shows the bulk-like optical constants n and k, which are input parameters for the AB-EMA approach and also compared to values obtained from a 100 nm solid Co thin film. The second row depicts the effective optical constants (n_{eff} and k_{eff}) along major axes of polarizability a, b, c, which are due to the different depolarization factors.

This shows that the film properties are not affected by storage in ambient air and expected aging effects due to material oxidation not present due to the Al_2O_3 passivation layer. The determined layer thickness t and slanting angle θ are in very good agreement with cross-section SEM analysis (Fig. 1). The Co film fraction f_{Co} is with 24% very low, which is characteristic for GLAD at very oblique angles.[8] The observed imbalance between f_{void} and $f_{Al_2O_3}$ as well as the slight changes in best-match Co bulk optical constants can be mainly attributed to differences in ambient humidity at the two measurement days. This is supported by the fact that there is virtually no effective optical constant variation along **c**. It is well-known that such nanostructured thin films are very sensitive high-speed capacitive humidity sensors.[21] In general, the depolarization factors render a biaxial material with column-like geometry extended along the c-axis: $L_c^D \ll L_a^D \sim L_b^D$. The wavelength-by-wavelength determined best-match Co bulk optical constants obtained from model analysis for the passivated Co SCTF after deposition and after 60 d are in excellent agreement with each other; however, differ from the ones determined for a 100 nm thin solid reference film grown in the same deposition chamber. This might be due to the idealized optical model as well as nanostructure confinement effects and the inherent large surface to volume ratio, which can affect the overall polarizability of the material. The effective optical properties only differ notably for $n_{eff,a}$ and $n_{eff,b}$, which indicates no material change due to oxidation ($n_{eff,c}$ unaffected), for example, but rather changes in the void regions caused by possible humidity changes. The investigation and quantification of water vapor adsorption in a controlled environment will be subject to a forthcoming publication.

The calculated Al_2O_3 shell layer thickness based on best-match AB-EMA constituent fraction parameters is with 2.4 nm in excellent agreement with the reference sample layer thickness of 3.29 nm. Note that for this calculation, ideal and separated nanocolumns with an average diameter of 17.5 nm are assumed. High resolution SEM top-view and cross-section image analysis show that the diameter of individual columns is increased by approximately 4 nm after ALD Al_2O_3 coating.

In summary, we have demonstrated that our generalized AB-EMA is an excellent approach to determine structural parameters as well as film fractions of multiple constituents of thin biaxial SCTFs with monoclinic optical properties. Furthermore, it was confirmed by spectroscopic Mueller matrix ellipsometry that a thin conformal Al_2O_3 ALD coating is suitable for passivation of metal SCTFs thereby preventing oxidation and aging effects. It is proposed that passivated three-dimensional sculptured thin films can be exploited as highly sensitive optical sensors, which may be analyzed by means of the presented AB-EMA approach to quantify sensed matter.

[1] O. Toader and S. John, Science **292**, 1133 (2001).
[2] S. V. Kesapragada, P. Victor, O. Nalamasu, and D. Gall, Nano Lett. **6**, 854 (2006).
[3] D. Schmidt, T. Hofmann, C. M. Herzinger, E. Schubert, and M. Schubert, Appl. Phys. Lett. **96**, 091906 (2010).
[4] M. Knez, K. Nielsch, and L. Niinistö, Adv. Mater. **19**, 3425 (2007).

[5] O. Albrecht, R. Zierold, S. Allende, J. Escrig, C. Patzig, B. Rauschenbach, K. Nielsch, and D. Görlitz, J. Appl. Phys. **109**, 093910 (2011).

[6] G. B. Smith, Opt. Commun. **71**, 279 (1989).

[7] C. G. Granqvist, D. L. Bellac, and G. A. Niklasson, Renewable Energy **8**, 530 (1996).

[8] G. Beydaghyan, C. Buzea, Y. Cui, C. Elliott, and K. Robbie, Appl. Phys. Lett. **87**, 153103 (2005).

[9] R. A. May, D. W. Flaherty, C. B. Mullins, and K. J. Stevenson, J. Phys. Chem. Lett. **1**, 1264 (2010).

[10] T. Hofmann, D. Schmidt, A. Boosalis, P. Kühne, R. Skomski, C. M. Herzinger, J. A. Woollam, M. Schubert, and E. Schubert, Appl. Phys. Lett. **99**, 081903 (2011).

[11] D. Schmidt, A. C. Kjerstad, T. Hofmann, R. Skomski, E. Schubert, and M. Schubert, J. Appl. Phys. **105**, 113508 (2009).

[12] C.-C. Wang, C.-C. Kei, Y.-W. Yu, and T.-P. Perng, Nano Lett. **7**, 1566 (2007).

[13] D. A. G. Bruggeman, Ann. Phys. (Leipzig) **24**, 636 (1935).

[14] D. Polder and J. H. van Santen, Physica **12**, 257 (1946).

[15] A. Shivola, *Electromagnetic Mixing Formulas and Applications, Electromagnetic Waves* (The Institution of Electrical Engineers, London, 1999), Vol. 47.

[16] M. Schubert, *Infrared Ellipsometry on Semiconductor Layer Structures: Phonons, Plasmons, and Polaritons, Springer Tracts in Modern Physics* (Springer, Berlin, 2004), Vol. 209.

[17] D. Schmidt, B. Booso, T. Hofmann, E. Schubert, A. Sarangan, and M. Schubert, Appl. Phys. Lett. **94**, 011914 (2009).

[18] D. Schmidt, B. Booso, T. Hofmann, E. Schubert, A. Sarangan, and M. Schubert, Opt. Lett. **34**, 992 (2009).

[19] M. de Graef and M. E. McHenry, *Structure of Materials: An Introduction to Crystallogrpahy, Diffraction, and Symmetry* (Cambridge University Press, Cambridge, 2007).

[20] See supplementary material at http://dx.doi.org/10.1063/1.3675549 for further details on model parameter uniqueness.

[21] J. J. Steele, M. Taschuk, and M. J. Brett, IEEE Sens. J. **8**, 1422 (2008).